Infrared Spectra and Density Functional Calculations of the Silver and Gold Thiocarbonyls: MCS, M(CS)2, and M2CS (M = Ag and Au) in Solid Argon

ARTICLE *in* THE JOURNAL OF PHYSICAL CHEMISTRY A · FEBRUARY 2004

Impact Factor: 2.69 · DOI: 10.1021/jp0374049

Infrared Spectra and Density Functional Calculations of the Silver and Gold Thiocarbonyls: MCS, $M(CS)_2$, and M_2CS (M = Ag and Au) in Solid Argon

Qingyu Kong,[†] Aihua Zeng,[†] Mohua Chen,[†] Qiang Xu,[‡] and Mingfei Zhou*[,†]

Shanghai Key Laboratory of Molecular Catalysts and Innovative Materials, Department of Chemistry, Fudan University, Shanghai 200433, P. R. China, and National Institute of Advanced Industrial Science and Technology (AIST), Ikeda, Osaka 563-8577, Japan

Received: November 7, 2003; In Final Form: December 17, 2003

Laser-ablated Ag and Au atoms have been reacted with high-frequency discharged CS_2 followed by condensation in excess argon at 4 K. Besides the known metal and carbon disulfide reaction products, binary silver and gold thiocarbonyls [MCS, $M(CS)_2$, and M_2CS (M = Ag and Au)] were formed via the reactions of ground-state metal atoms or dimers with CS in solid argon. The product absorptions were identified by isotopic substitutions and density functional calculations. This work provides the first vibrational spectroscopic characterization of the binary Ag and Au thiocarbonyl complexes.

Introduction

Carbon monoxide and carbon monosulfide are isovalent molecules. Both are very common and important ligands in organometallic chemistry. Although a very large number of binary transition metal carbonyl complexes have been well-studied,[1] analogous transition metal thiocarbonyl complexes have received far less attention, partly because of the lack of the stable molecular CS.[2] Previous theoretical investigations have shown that the bonding mechanisms on transition metal monothiocarbonyls and monocarbonyls are similar, but the thiocarbonyls are much more strongly bound than the corresponding carbonyls.[3]

Experimentally, the CS molecules can be prepared with discharge of the CS_2 molecules.[4,5] By co-deposition of microwave discharged CS_2 and argon mixture with thermal evaporated nickel atoms, $Ni(CS)_4$ has been first synthesized and characterized in solid argon.[5] Recently, we reported matrix isolation infrared absorption spectra of binary copper thiocarbonyls: CuCS, $Cu(CS)_2$, and Cu_2CS, which were produced by the reactions of copper atoms with CS molecules generated via high-frequency discharge of CS_2 vapor in excess argon.[6] In this paper, we report a similar matrix isolation FTIR spectroscopic and density functional theoretical investigation of the silver and gold thiocarbonyls.

Experimental and Theoretical Methods

The CS molecules were prepared by subjecting CS_2/Ar mixtures to high-frequency discharge with a high-frequency generator (Tesla coil).[4] The tip of the Tesla coil was connected to a copper cap on one end of a quartz tube extending into the vacuum chamber. The other end of the quartz tube was connected to a copper tube with ground potential. Discharge takes place between the cap and the copper tube. CS_2/Ar mixtures were prepared in a stainless steel vacuum line using standard manometric technique. CS_2 was cooled to 77 K with liquid N_2 and evacuated to remove volatile impurities.

The experimental setup for pulsed laser ablation and matrix isolation FTIR spectroscopic investigation has been described in detail previously.[6,7] Briefly, the 1064-nm fundamental of a Nd:YAG laser (10 Hz repetition rate and 8 ns pulse width) was focused onto the rotating silver or gold metal target through a hole in a CsI window. The laser-ablated metal atoms were co-deposited with the Tesla coil discharged CS_2/Ar sample onto the 4 K CsI window for 1 h at a rate of 3−5 mmol/h. Infrared spectra were recorded on a Bruker Equinox 55 spectrometer at 0.5 cm^{-1} resolution with a DTGS detector. Matrix samples were annealed at different temperatures, and selected samples were subjected to broadband irradiation with use of a high-pressure mercury arc lamp.

Density functional theoretical calculations were performed with the Gaussian 98 program.[8] The most popular Becke three-parameter hybrid functional with the Lee−Yang−Parr correlation corrections (B3LYP) was used.[9,10] Previous work has shown that this hybrid functional can provide very reliable predictions of the state energies, structures, and vibrational frequencies of transition metal containing compounds.[11] For instance, the B3LYP functional worked well for binding energies and vibrational frequencies of the copper, silver, and gold carbonyls.[12,13] The 6-311+G* basis set for C and S atoms and the Los Alamos ECP plus DZ basis sets for Ag and Au atoms were used.[14] For comparison, calculations were also performed with the BPW91 functional as well.[15] Geometries were fully optimized and vibrational frequencies calculated with analytical second derivatives, and zero point vibrational energies were derived.

Results

Infrared Spectra. Our recent study has shown that high-frequency discharge of CS_2 vapor readily produces CS molecules.[6] Compared to the experiments without discharge, the integrated intensity of the CS_2 absorption at 1528.3 cm^{-1} decreased by about 30% in discharge experiments. Therefore, the concentration of CS in solid argon was roughly estimated to be about 0.15% when a 0.5% CS_2/Ar sample was used. The

* Author to whom correspondence should be addressed. E-mail: mfzhou@fudan.edu.cn.

[†] Fudan University.

[‡] National Institute of Advanced Industrial Science and Technology (AIST).

10.1021/jp0374049 CCC: $27.50
Published on Web 02/04/2004

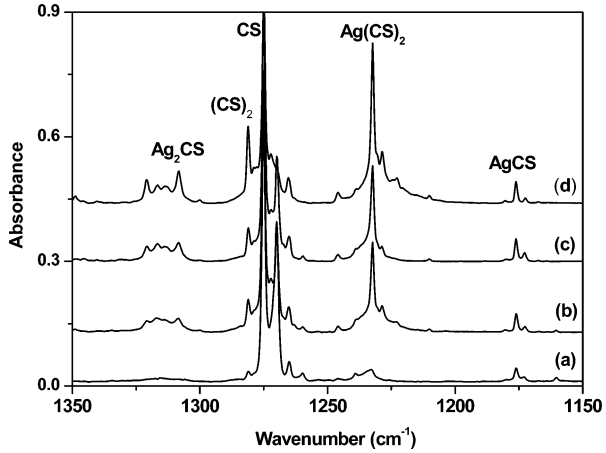

Figure 1. Infrared spectra in the 1350−1150 cm^{-1} region from co-deposition of laser-ablated silver atoms with discharged 0.5% CS_2/Ar sample: (a) 1 h sample deposition at 4 K, (b) after annealing to 30 K, (c) after 20 min of broadband irradiation, and (d) after annealing to 40 K.

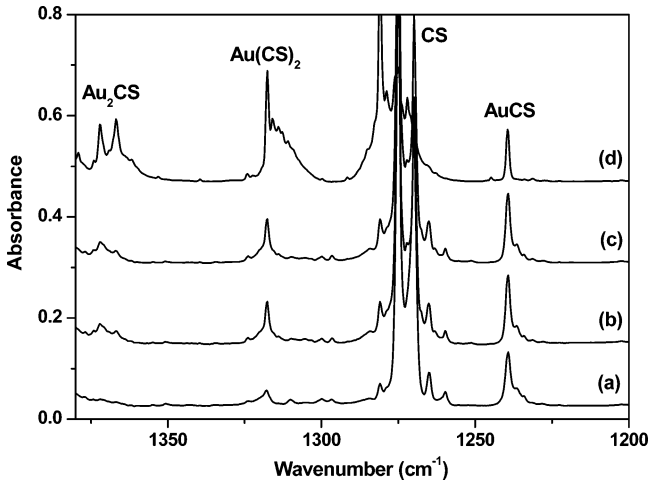

Figure 2. Infrared spectra in the 1380−1200 cm^{-1} region from co-deposition of laser-ablated gold atoms with discharged 0.5% CS_2/Ar sample: (a) 1 h sample deposition at 4 K, (b) after annealing to 30 K, (c) after 20 min of broadband irradiation, and (d) after annealing to 40 K.

TABLE 1: Infrared Absorptions from Co-deposition of Laser-Ablated Silver and Gold Atoms with Discharged CS_2/Ar Sample

$^{12}CS_2$	$^{13}CS_2$	$^{12}CS_2 + {}^{13}CS_2$	*R*(12/13)	assignment
1176.1	1142.4	1176.1, 1142.4	1.0295	AgCS
2553.3	2476.3	2553.3, 2516.8, 2476.3	1.0311	$Ag(CS)_2$
1232.3	1194.9	1232.3, 1210.1, 1194.9	1.0313	$Ag(CS)_2$
1308.2	1268.9	1308.2, 1268.9	1.0310	Ag_2CS
1320.8	1280.7	1320.8, 1280.7	1.0313	Ag_2CS site
1239.5	1202.4	1239.5, 1202.4	1.0309	AuCS
2698.7	2614.0	2698.7, 2659.5, 2614.0	1.0324	$Au(CS)_2$
1317.6	1276.6	1317.6, 1291.6, 1276.6	1.0321	$Au(CS)_2$
1366.8	1323.7	1366.8, 1323.7	1.0326	Au_2CS
1372.1	1328.7	1372.1, 1328.7	1.0327	Au_2CS site

infrared spectra in selected regions from co-deposition of laser-ablated Ag and Au atoms with discharged CS_2/Ar (0.5%) sample in excess argon are shown in Figures 1 and 2, and the product absorptions are listed in Table 1. Bands common to other CS_2 discharge experiments including $(CS)_2$, C_2S_2, CS_2^-, C_3S_2, and $S(CS)_2$ are omitted.[4,16] Similar to the recently reported metal + CS_2 reactions,[17] the AgSCS (1507.1 cm^{-1}, not shown) and AuSCS (1485.9 cm^{-1}, not shown) absorptions were observed on sample deposition and increased markedly on annealing.

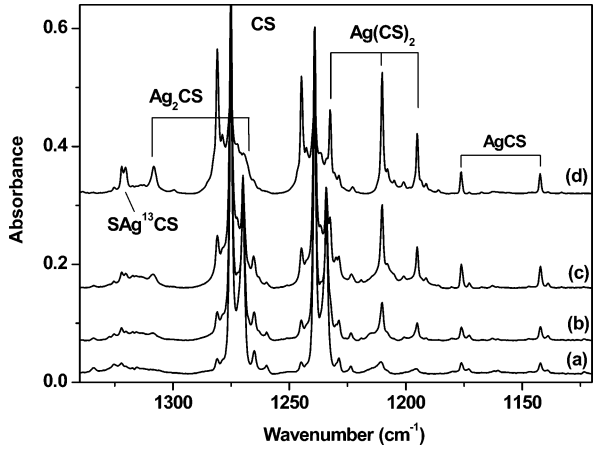

Figure 3. Infrared spectra in the 1340−1120 cm^{-1} region from co-deposition of laser-ablated silver atoms with discharged 0.25% $^{12}CS_2$ + 0.25% $^{13}CS_2$/Ar sample: (a) 1 h sample deposition at 4 K, (b) after annealing to 25 K, (c) after annealing to 30 K, and (d) after annealing to 35 K.

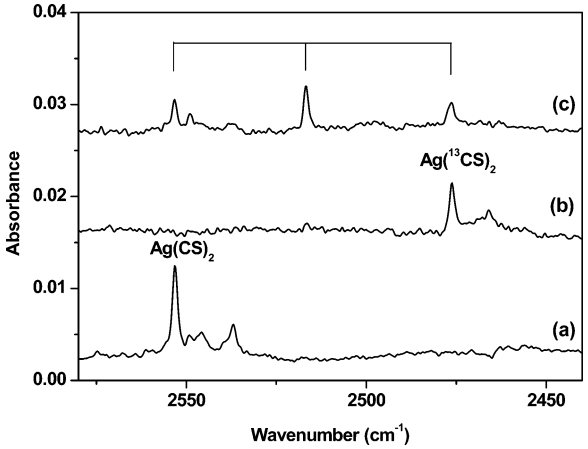

Figure 4. Infrared spectra in the 2580−2440 cm^{-1} region showing the combination bands of $Ag(CS)_2$: (a) discharged 0.5% CS_2/Ar, (b) discharged 0.5% $^{13}CS_2$/Ar, and (c) discharged 0.25% $^{12}CS_2$ + 0.25% $^{13}CS_2$/Ar.

Broadband irradiation destroyed these complex absorptions and produced the SAgCS (1362.2 cm^{-1}, not shown) and SAuCS (1382.1 cm^{-1}, not shown) absorptions. Besides these metal + CS_2 reaction products, new product absorptions also were observed as listed in Table 1. Different temperature annealing and broadband irradiation were demonstrated in Figures 1 and 2 to characterize the absorption species.

The experiments were repeated with isotopically labeled $^{13}CS_2$ and a $^{12}CS_2$ + $^{13}CS_2$ mixture. The spectra in selected regions are shown in Figures 3−5, and the absorptions are summarized in Table 1.

Calculation Results. DFT calculations were done for the potential product molecules with use of the B3LYP functional to be consistent with previous MCO and CuCS calculations.[6,12,13] The optimized structures are shown in Figures 6 and 7, and the calculated vibrational frequencies and intensities are summarized in Table 2.

Discussion

The new absorptions listed in Table 1 were produced only in the discharged experiments, which suggest that these absorptions are most likely contributed by the metal and CS reaction products, and will be identified as silver and gold thiocarbonyl complexes.

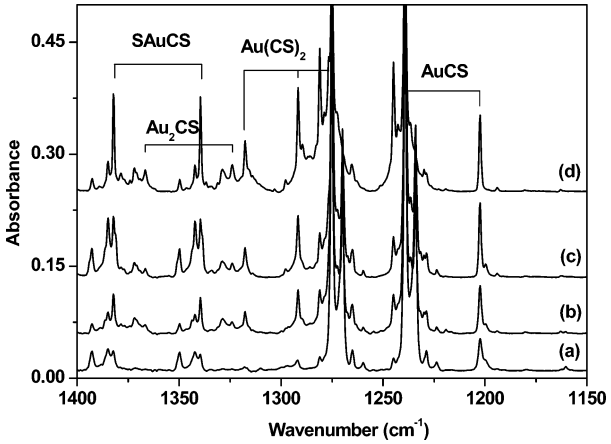

Figure 5. Infrared spectra in the 1400−1150 cm^{-1} region from co-deposition of laser-ablated gold atoms with discharged 0.25% $^{12}CS_2$ + 0.25% $^{13}CS_2$/Ar sample: (a) 1 h sample deposition at 4 K, (b) after annealing to 30 K, (c) after 20 min of broadband irradiation, and (d) after annealing to 35 K.

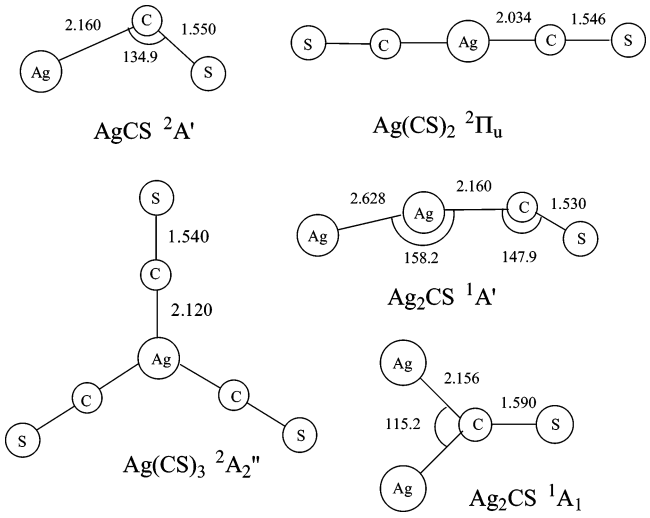

Figure 6. Optimized (B3LYP) structures of the $Ag(CS)_x$ ($x = 1-3$) and Ag_2CS molecules (bond length in Å, bond angle in deg).

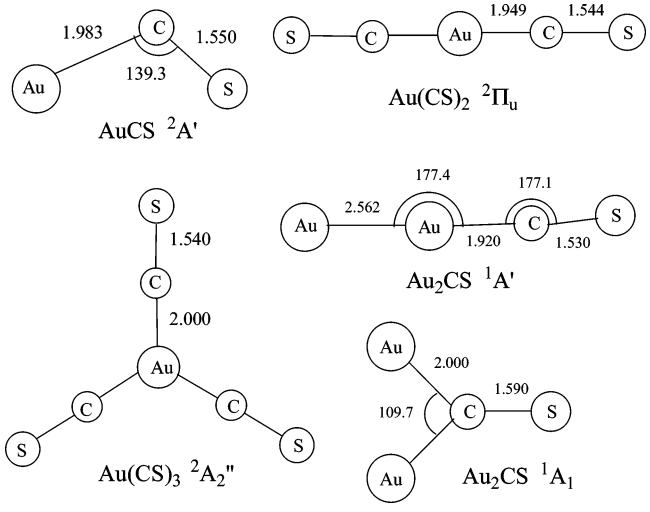

Figure 7. Optimized (B3LYP) structures of the $Au(CS)_x$ ($x = 1-3$) and Au_2CS molecules (bond length in Å, bond angle in deg).

AgCS. As shown in Figure 1, absorption at 1176.1 cm^{-1} is weak on sample deposition, and increased on annealing. This band shifted to 1142.4 cm^{-1} with $^{13}CS_2$. The $^{12}C/^{13}C$ isotopic frequency ratio of 1.0295 suggests a C−S stretching vibration of the thiocarbonyl complex. In the mixed $^{12}CS_2$ + $^{13}CS_2$ experiment (Figure 3), only the 1176.1- and 1142.4-cm^{-1} bands were observed, indicating that only one CS is involved in this mode. Therefore, we assign the 1176.1-cm^{-1} band to the C−S stretching vibration of AgCS.

TABLE 2: Calculated (B3LYP) Vibrational Frequencies (cm^{-1}) and Intensities (km/mol) for MCS, $M(CS)_2$, $Ag(CS)_3$, and M_2CS (M = Ag and Au)

	frequency (intensity)
AgCS ($^2A'$)	1216.4 (746), 309.8 (12), 138.1 (8)
AgCS ($^2\Sigma^+$)[a]	1322.7 (181), 402.2 (106), 85.8 (4)
$Ag(CS)_2$ ($^2\Pi_u$)	1353.5 (0), 1297.5 (2650), 330.7 (16), 292.6 (23), 250.9 (0), 239.2 (6), 206.0 (0), 38.0 (0)
Ag_2CS ($^1A'$)	1304.3 (735), 267.1 (22), 171.4 (10), 134.8 (11), 132.7 (1), 28.5 (3)
$Ag(CS)_3$ ($^2A_2''$)	1330.8 (0), 1271.5 (4506), 284.1 (0), 211.4 (7), 198.2 (0), 192.2 (2), 167.1 (0), 143.6 (0), 24.4 (1), 20.9 (1)
AuCS ($^2A'$)	1240.7 (561), 425.3 (8), 184.3 (13)
AuCS ($^2\Sigma^+$)[b]	1334.0 (348), 254.4 (0), 1152.8i (2140)
$Au(CS)_2$ ($^2\Pi_u$)	1407.5 (0), 1340.5 (1646), 392.7 (9), 332.7 (28), 331.3 (0), 307.4 (2), 258.9 (0), 44.0 (1)
Au_2CS ($^1A'$)	1398.8 (534), 341.7 (0), 305.7 (0), 302.7 (0), 161.5 (7), 34.0 (1)

[a] Ag−C: 2.447 Å. C−S: 1.533 Å. [b] Au−C: 2.010 Å. C−S: 1.535 Å.

The assignment is supported by density functional calculations. Our DFT/B3LYP calculation found a $^2A'$ ground state with a strong C−S stretching vibration at 1216.4 cm^{-1}, which is 40.3 cm^{-1} higher than the observed value. The calculated $^{12}C/^{13}C$ isotopic frequency ratio of 1.0295 fits the experimental value very well. The Ag−C stretching and the bending modes of AgCS were predicted to absorb below 400 cm^{-1} with much lower intensity than that of the CS stretching mode. The linear structure ($^2\Sigma^+$) was predicted to be 12.2 kcal/mol higher in energy than the bent structure. The C−S stretching frequency in the linear structure was calculated at 1322.7 cm^{-1}.

AuCS. Similar absorption at 1239.5 cm^{-1} in the gold experiments (Figure 2) is assigned to the AuCS molecule. This band was observed on sample deposition, increased slightly on 30 K annealing, but decreased on 40 K annealing. It shifted to 1202.4 cm^{-1} with $^{13}CS_2$, and gave a $^{12}C/^{13}C$ isotopic frequency ratio of 1.0309. This ratio is indicative of a terminal CS stretching vibration. As shown in Figure 5, only the pure isotopic counterparts were presented in the mixed $^{12}CS_2$ + $^{13}CS_2$ experiment, indicating that only one CS subunit is involved in the mode. The assignment is confirmed by DFT/B3LYP calculations, which found a bent $^2A'$ ground state with a strong C−S stretching vibration at 1240.7 cm^{-1} with a $^{12}C/^{13}C$ isotopic frequency ratio of 1.0305. The linear structure ($^2\Sigma^+$) was predicted to be 9.4 kcal/mol higher in energy than the bent structure, and is only a transition state based on the presence of negative calculated bending frequency.

In transition metal carbonyls, the interactions between metal and ligand CO are dominated by the synergic donation of electrons in 5σ HOMO of CO to an empty symmetry matching orbital of the metal and the back-donation of the metal π electrons to the CO π^* orbital. Similarly, thiocarbonyls are formed by the interactions of metal with CS. The ground state of AgCS and AuCS correlates to the ground-state metal atom with the $d^{10}\,s^1$ electronic configuration. Analogous to the CuCS and CuCO molecules,[6,12,18] both the AgCS and AuCS monothiocarbonyls prefer a bent geometry to reduce the repulsion between the metal valence s and the CS 7σ orbitals. The bond angles of AgCS and AuCS were predicted to be 134.9°and 139.3°.

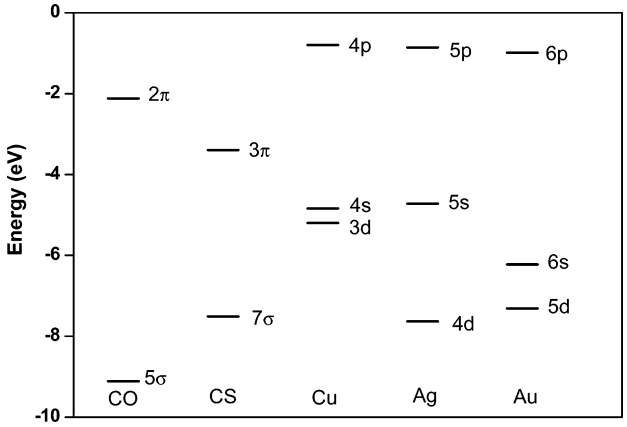

Figure 8. The energy levels of the valence orbitals of CO, CS, Cu, Ag, and Au calculated with the BPW91 functional.

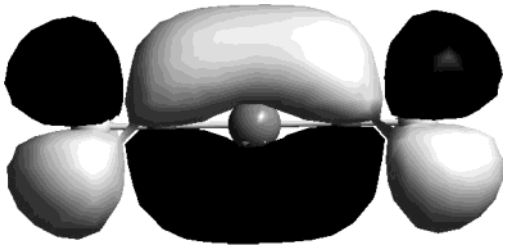

Figure 9. Depiction of the highest occupied molecular orbital (π_u) of $Ag(CS)_2$.

The binding energies of AgCS and AuCS were computed to be 12.8 and 25.6 kcal/mol with respect to their dissociation limits: ground-state metal atom and CS. In our recent study, the binding energy of CuCS was predicted to be 26.9 cal/mol at the B3LYP/6-311+G* level.[6] The binding energies of CuCS and AuCS are very close, while the binding energy of AgCS is significantly lower than that of CuCS and AuCS. However, the binding energies of these thiocarbonyls are significantly larger than that of the corresponding metal monocarbonyls. Both copper and gold monocarbonyls are stable and have been experimentally characterized.[12,13,19,20] The binding energies of CuCO and AuCO were predicted to be 7.4 and 7.6 kcal/mol. Silver is the only transition metal that failed to form the stable binary monocarbonyl. Although earlier researchers claimed the existence of the silver monocarbonyl in rare gas matrices,[21] no evidence of the isolated silver monocarbonyl was found in the later experiments.[13,22,23] The matrix ESR and theoretical studies showed that silver monocarbonyl is not a stable complex.[23,24] Kasai and Jones discussed in detail the relative stability of the copper, silver, and gold monocarbonlys based on energy levels of the valence $(n-1)$d, *n*s, and *n*p orbitals of the Cu, Ag, and Au atoms and those of the lone pair 5σ and vacant π^* orbitals of CO.[23] Figure 8 shows schematically the energy levels of the valence orbitals of the metal atoms and those of the 5σ or 7σ lone pair and the vacant 2π or 3π antibonding orbitals of CO and CS calculated with the BPW91 functional. The energy separation between the Cu 3d and CO π^* levels is smaller than the separation between the Cu 4s and CO 5σ orbitals, the σ donation is small, and the π back-donation is primarily responsible for the formation of CuCO. The Ag 5s and 5p orbitals are virtually at the same energy levels as those of Cu, but the energy level of the Ag 4d orbital is about 2.4 eV lower in energy than that of the Cu 3d orbital. The extra stability of the Ag 4d orbital blocks the back-donation occurrence and thus makes the AgCO molecule unbound. In the case of Au, the metal 5d is between Cu and Ag, but the metal s orbital is much closer to the CO 5σ than for Cu and Ag. Hence, AuCO is a stable complex. The energy level of the 7σ HOMO of CS is higher than that of the 5σ HOMO of CO, whereas the energy level of the π^* LOMO of CS is lower than that of the π^* LUMO of CO, and therefore, thiocarbonyls have significantly more σ donation and π back-donation than those of the corresponding carbonyls. Thus, the monothiocarbonyls are more strongly bound than the monocarbonyls and AgCS is a stable complex.

$Ag(CS)_2$. The next band observed to markedly gain intensity on first annealing is at 1232.3 cm^{-1}. Annealing to high temperature (35 and 40 K) produced more of the 1232.3-cm^{-1} band (Figure 1). This band dominated the spectrum after 35 K annealing, and is favored in the experiments with high CS_2 concentrations. This band shifted to 1194.9 cm^{-1} with $^{13}CS_2$. The $^{12}C/^{13}C$ isotopic frequency ratio of 1.0313 is indicative of a C−S stretching vibration. The 1232.3-cm^{-1} band formed a sharp triplet pattern at 1232.3, 1210.1, and 1194.9 cm^{-1} with approximately 1:2:1 relative intensities with the $^{12}CS_2$ and $^{13}CS_2$ mixture (Figure 3), which indicates the vibration of two equivalent CS subgroups. The $Ag(CS)_2$ molecule is the most likely absorber. The intermediate component for $Ag(^{12}CS)(^{13}CS)$ is 3.5 cm^{-1} lower than the means of pure isotopic frequencies, which points to a higher frequency symmetric C−S stretching mode. The pure isotopic symmetric stretching mode is not observed here, which suggests that $Ag(CS)_2$ is a linear molecule.

An associated weaker absorption at 2553.3 cm^{-1} was observed with approximately 4% of the intensity of the 1232.3-cm^{-1} band, and is due to a combination band. The $^{13}CS_2$ counterpart was observed at 2476.3 cm^{-1}, and triplet mixed isotopic bands were clearly observed at 2553.3, 2516.6, and 2476.3 cm^{-1} in the $^{12}CS_2 + {}^{13}CS_2$ experiment (Figure 4). The 2553.3-cm^{-1} band is separated from the 1232.3-cm^{-1} band by 1321.0 cm^{-1}. Analogous separations of 1306.5 and 1281.3 cm^{-1} were deduced for the $Ag(^{12}CS)(^{13}CS)$ and $Ag(^{13}CS)_2$ bands, respectively. These frequency separations and the deduced $^{12}C/^{13}C$ isotopic frequency ratio of 1.0310 are appropriate for a symmetric C−S stretching vibration. Taking the anharmonicity into consideration, the symmetric C−S stretching mode of $Ag(CS)_2$ should be some 20 cm^{-1} higher near 1340 cm^{-1}.[25]

The $Ag(CS)_2$ molecule was predicted to have a $^2\Pi_u$ ground state with linear structure (Figure 6). Geometry optimization on a bent structure converged to the linear structure. The antisymmetric and symmetric C−S stretching modes were computed at 1297.5 and 1353.5 cm^{-1} with $^{12}C/^{13}C$ isotopic ratios of 1.0315 and 1.0316, respectively, in good agreement with the experimentally determined values. The antisymmetric CS stretching mode has the largest IR intensity (2650 km/mol versus less than 23 km/mol for the other modes). The symmetric CS stretching mode is IR inactive, but this mode of the $Ag(^{12}CS)(^{13}CS)$ molecule is IR active because of the reduced symmetry. It was predicted at 1339.4 cm^{-1} with an IR intensity of 273 km/mol. This band could either be too weak to be observed or be overlapped by the strong $SAg^{13}CS$ or Ag_2CS absorptions.

$Au(CS)_2$. Similar bands at 1317.6 and 2698.7 cm^{-1} in the gold reaction are assigned to the antisymmetric CS stretching and the combination of symmetric and antisymmetric CS stretching modes of the linear $Au(CS)_2$ molecule following the example of $Ag(CS)_2$. These bands are weak on sample deposition and greatly increased on annealing (Figure 2). The 1317.6-cm^{-1} band shifted to 1276.6 cm^{-1} with $^{13}CS_2$ and gave a $^{12}C/^{13}C$ isotopic ratio of 1.0321. In the mixed $^{12}CS_2 + {}^{13}CS_2$ experiment, a triplet at 1317.6, 1291.6, and 1276.6 cm^{-1} with approximately 1:2:1 relative intensity was observed (Figure 5),

indicating that two equivalent CS subgroups are involved in this mode. The 2698.7-cm^{-1} band is much weaker than the 1317.6-cm^{-1} band, and a similar triplet was observed at 2698.7, 2659.5, and 2614.0 cm^{-1} in the mixed $^{12}CS_2 + {}^{13}CS_2$ experiment. The 2698.7-cm^{-1} absorption is 1381.1 cm^{-1} above the strong 1317.6-cm^{-1} band, and the ^{13}CS counterpart is separated by 1337.4 cm^{-1}. These intervals are appropriate for a symmetric CS stretching mode of $Au(CS)_2$.

The $Au(CS)_2$ molecule also has a $^2\Pi_u$ ground state with linear structure as shown in Figure 7. The antisymmetric and symmetric C−S stretching modes were computed at 1340.5 and 1407.5 cm^{-1} with $^{12}C/^{13}C$ isotopic ratios of 1.0321 and 1.0330, respectively. The stretching frequencies and isotopic frequency ratios are in good agreement with the experimental values.

For the dithiocarbonyls, the bonding is different from that of the monothiocarbonyls. Due to the extra stability of the filled nd^{10} shell of the metal, s-to-d promotion is not favored. Since metal s-to-p promotion requires quite large energy, the monothiocarbonyls possess bent geometry that correlates to the ground-state metal atoms. In the case of dithiocarbonyls, however, there are two CS molecules to share the cost of s-to-p promotion, the ground state of dithiocarbonyls correlates to the first excited state of the metal atom with the $d^{10}\ s^0\ p^1$ electronic configuration. The s-to-p promotion significantly reduces the σ repulsion and increases the metal-to-CS π back-donation. All the $M(CS)_2$ (M = Cu, Ag, and Au) molecules are linear. The molecules prefer the linear geometry to maximize the metal-to-CS bonding. The π back-donation of Ag-to-CS π^* is shown clearly in the HOMO (π_u) of $Ag(CS)_2$. The dithiocarbonyls are more strongly bound than the monothiocarbonyls. The metal−C bond lengths of the $Cu(CS)_2$, $Ag(CS)_2$, and $Au(CS)_2$ dithiocarbonyls were calculated to be 1.830, 2.034, and 1.949 Å, respectively, shorter than that of the corresponding monothiocarbonyls (1.875, 2.160, and 1.983 Å). The binding energies of the second CS were estimated to be 49.5, 30.4, and 44.4 kcal/mol, after zero-point energy correction, which are much higher than that of the CuCS (26.9 kcal/mol),[6] AgCS (12.8 kcal/mol), and AuCS (25.6 kcal/mol) monothiocarbonyls. The order of relative stability of dithiocarbonyls is the same as that of the monothiocarbonyls and the dicarbonyls: Cu ≈ Au > Ag. The $M(CO)_2$ (M = Cu, Ag, and Au) dicarbonyls all are stable and have been experimentally characterized. The dicarbonyls all have $^2\Pi_u$ ground states with linear symmetry.[12,13] The binding energies of the second CO were calculated to be 18.2, 1.6, and 11.5 kcal/mol, respectively, after zero-point energy correction. Apparently, the bonding of dicarbonyls is significantly weaker than that of the dithiocarbonyls.

Ag_2CS. In the Ag experiments, a band at 1308.2 cm^{-1} appeared on first annealing and increased on subsequent high-temperature annealing. This band shifted to 1268.9 cm^{-1} upon replacing $^{12}CS_2$ by $^{13}CS_2$. The $^{12}C/^{13}C$ isotopic frequency ratio of 1.0310 implies that the band is due to a CS stretching vibration of thiocarbonyl. In the mixed $^{12}CS_2 + {}^{13}CS_2$ experiment, no obvious intermediate component was observed, indicating that only one CS subgroup is involved in this mode. This band appeared after the AgCS absorption on annealing, and the band intensity is large with high laser power relative to the AgCS and $Ag(CS)_2$ absorptions. Accordingly, we assign the 1308.2-cm^{-1} band to the CS stretching vibration of the Ag_2CS molecule. The band position suggests that the Ag_2CS molecule has an end-on instead of a bridged structure.

The assignment is supported by DFT calculations. As shown in Figure 6, the ground state of Ag_2CS was calculated to be $^1A'$ with an end-on structure. The bridged structure with CS bonded to both the two silver atoms was predicted to be 15.3 kcal/mol higher in energy than the end-on structure. The CS stretching frequency for the ground-state Ag_2CS molecule was calculated at 1304.3 cm^{-1}, just 3.9 cm^{-1} lower than the observed value. The bridged structure of Ag_2CS was predicted to absorb at 1105.3 cm^{-1}, which is too low to fit the observed frequency.

Au_2CS. A similar band at 1366.8 cm^{-1} in the gold experiment is assigned to the Au_2CS molecule. The ^{13}CS counterpart was observed at 1323.7 cm^{-1}. The ground state of Au_2CS was predicted to be $^1A'$ with an end-on structure. The CS stretching frequency and isotopic frequency ratio were computed to be 1398.8 cm^{-1} and 1.0320.

The bonding of M_2CS (M = Cu, Ag, and Au) is very similar to that of other metal dimer complexes such as Cu_2CO, Fe_2CO, and Co_2CO,[26−28] and also involves the usual donation/back-donation mechanism. The Cu_2, Ag_2, and Au_2 dimers were predicted to have the $^1\Sigma_g^+$ ground state. The $^1A'$ ground-state M_2CS complexes correlate with the $^1\Sigma_g^+$ ground state of the metal dimer and CS. To reduce the repulsion between the filled σ molecular orbital of metal dimer and CS, the M_2CS complexes are bent analogous to the MCS monothiocarbonyl complexes. The MMC and MCS bond angles were calculated to be 165.1 and 163.5° (Cu),[5] 158.2 and 147.9° (Ag), and 177.4 and 177.1° (Au), respectively. Previous theoretical studies pointed out that the repulsion decreases from metal-to-metal dimer because of charge accumulation in the metal−metal midbond region and of the greater polarization of metal dimer.[25] Replacing the terminal metal atom in M_2CS with more electronegative atoms such as sulfur could further reduce the repulsion. The resulting SMCS molecules were linear as predicted by DFT calculations.[17,29] The binding energies of M_2CS were computed to be 28.2 (Cu), 12.5 (Ag), and 39.9 kcal/mol (Au), respectively, with respect to their dissociation limits: ground state M_2 + CS.

No evidence was found for the formation of the trithiocarbonyl species in the present experiments. The $Cu(CS)_3$ molecule was not observed in the Cu reaction either.[6] Both the $Cu(CO)_3$ and $Ag(CO)_3$ molecules have been observed in solid matrix,[12,13] which suggests that $Cu(CS)_3$ and $Ag(CS)_3$ also should be observable. Our DFT calculations predicted that $Cu(CS)_3$, $Ag(CS)_3$, and $Au(CS)_3$ all have $^2A_2''$ ground state with planar D_{3h} symmetry. The $Au(CS)_3$ molecule was predicted to be unbound with respect to $Au(CS)_2$ + CS, the same as the $Au(CO)_3$ carbonyl. However, both the $Cu(CS)_3$ and $Ag(CS)_3$ molecules were predicted to be stable with respect to $Cu(CS)_2$ + CS and $Ag(CS)_2$ + CS. The binding energies of the third CS were calculated to be 6.1 kcal/mol for $Ag(CS)_3$ with the B3LYP functional. Similar calculations with the BPW91 functional gave a value of 10.1 kcal/mol. One possible explanation is that the trithiocarbonyl absorptions may be overlapped by the strong and broad CS absorptions.

Silver and gold carbonyl cations were observed in the reactions of laser-ablated silver and gold atoms with CO in excess neon.[13] Weak CS_2^- absorption was observed in the present experiments, but no evidence of the thiocarbonyl cation was found.

Conclusions

Silver and gold thiocarbonyl complexes MCS, $M(CS)_2$, and M_2CS (M = Ag and Au) have been studied by matrix isolation infrared absorption spectroscopy and density functional theory calculations. These metal thiocarbonyl complexes were produced by the reactions of CS produced by high-frequency discharge and metal atoms or dimers in solid argon matrix.

The bonding in these thiocarbonyls is very similar to that in the corresponding carbonyls, and is dominated by the synergic

donation of electrons in the 7σ HOMO of CS to an empty symmetry matching orbital of the metal and the back-donation of the metal π electrons to the CS π^* orbital. The metal atoms have $(n-1)d^{10}\ ns^1$ electronic configuration, the s-to-d promotion is not possible, so s-to-p promotion takes place instead. However, the energy difference between s and p orbitals is large, and hence, the ground state of monothiocarbonyls correlates to the ground-state metal atom and prefers a bent geometry to reduce the repulsion between the metal valence s and the CS 7σ orbitals. There are two CS molecules to share the cost of s-to-p promotion, the ground state of dithiocarbonyls correlates to the first excited state of the metal atom with the $d^{10}\ s^0\ p^1$ electronic configuration. The dithiocarbonyls are linear and more strongly bound than the monothiocarbonyls.

In the Cu, Ag, and Au group carbonyls and thiocarbonyls, the bonding in thiocarbonyls is stronger than that in the corresponding carbonyls, and the bonding between silver and CS is much weaker than that of copper and gold. These differences can be understood based on the energy differences between valence d, s, and p orbitals of the metal atoms, as well as the σ HOMO and π^* LUMO of CO and CS.

Acknowledgment. We greatly acknowledge financial support from NSFC (20125033) and the NKBRSF of China.

References and Notes

(1) Cotton, F. A.; Wilkinson, G.; Murillo, C. A.; Bochmann, M. *Advanced Inorganic Chemistry*, 6th ed.; Wiley: New York, 1999. Falbe, J. *Carbon monoxide in Organic Synthesis*; Springer-Verlag: Berlin, Germany, 1980. Zhou, M. F.; Andrews, L.; Bauschlicher, C. W., Jr. *Chem. Rev*. **2001**, *101*, 1931.

(2) Broadhurst, P. V. *Polyhedron* **1985**, *4*, 1801. Butler, I. S. *Acc. Chem. Res*. **1977**, *10*, 359.

(3) Jeung, G. H. *J. Am. Chem. Soc.* **1992**, *114*, 3211.

(4) Bohn, R. B.; Hannachi, Y.; Andrews, L. *J. Am. Chem. Soc.* **1992**, *114*, 6452.

(5) Calder, G. V.; Verkade, J. G.; Yarbrough, L. W. *J. Chem. Soc., Chem. Commun*. **1973**, 705.

(6) Kong, Q. Y.; Zeng, A. H.; Chen, M. H.; Zhou, M. F.; Xu, Q. *J. Chem. Phys.* **2003**, *118*, 7267.

(7) Chen, M. H.; Wang, X. F.; Zhang, L. N.; Yu, M.; Qin, Q. Z. *Chem. Phys.* **1999**, *242*, 81. Zhou, M. F.; Zhang, L. N.; Qin, Q. Z. *J. Am. Chem. Soc.* **2000**, *122*, 4483.

(8) Frisch, M. J.; Trucks, G. W.; Schlegel, H. B.; Scuseria, G. E.; Robb, M. A.; Cheeseman, J. R.; Zakrzewski, V. G.; Montgomery, J. A., Jr.; Stratmann, R. E.; Burant, J. C.; Dapprich, S.; Millam, J. M.; Daniels, A. D.; Kudin, K. N.; Strain, M. C.; Farkas, O.; Tomasi, J.; Barone, V.; Cossi, M.; Cammi, R.; Mennucci, B.; Pomelli, C.; Adamo, C.; Clifford, S.; Ochterski, J.; Petersson, G. A.; Ayala, P. Y.; Cui, Q.; Morokuma, K.; Malick, D. K.; Rabuck, A. D.; Raghavachari, K.; Foresman, J. B.; Cioslowski, J.; Ortiz, J. V.; Baboul, A. G.; Stefanov, B. B.; Liu, G.; Liashenko, A.; Piskorz, P.; Komaromi, I.; Gomperts, R.; Martin, R. L.; Fox, D. J.; Keith, T.; Al-Laham, M. A.; Peng, C. Y.; Nanayakkara, A.; Gonzalez, C.; Challacombe, M.; Gill, P. M. W.; Johnson, B.; Chen, W.; Wong, M. W.; Andres, J. L.; Gonzalez, C.; Head-Gordon, M.; Replogle, E. S.; Pople, J. A. *Gaussian 98*, Revision A.7; Gaussian, Inc.: Pittsburgh, PA, 1998.

(9) Becke, A. D. *J. Chem. Phys.* **1993**, *98*, 5648.

(10) Lee, C.; Yang, E.; Parr, R. G. *Phys. Rev. B* **1988**, *37*, 785.

(11) Bauschlicher, C. W., Jr.; Ricca, A.; Partridge, H.; Langhoff, S. R. In *Recent Advances in Density Functional Theory*; Chong, D. P., Ed.; World Scientific Publishing: Singapore, 1997; Part II. Siegbahn, P. E. M. Electronic Structure Calculations for Molecules Containing Transition Metals. *Adv. Chem. Phys.* **1996**, 93. Bytheway, I.; Wong, M. W. *Chem. Phys. Lett.* **1998**, *282*, 219.

(12) Zhou, M. F.; Andrews, L. *J. Chem. Phys*. **1999**, 111, 4548.

(13) Liang, B. Y.; Andrews, L. *J. Phys. Chem. A* **2000**, *104*, 9156.

(14) McLean, A. D.; Chandler, G. S. *J. Chem. Phys.* **1980**, *72*, 5639. Krishnan, R.; Binkley, J. S.; Seeger, R.; Pople, J. A. *J. Chem. Phys.* **1980**, *72*, 650. Hay, P. J.; Wadt, W. R. *J. Chem. Phys.* **1985**, *82*, 270. Wadt, W. R.; Hay, P. J. *J. Chem. Phys.* **1985**, *82*, 284.

(15) Perdew, J. P.; Wang, Y. *Phys. Rev. B* **1992**, 45, 13244.

(16) Jacox, M. E.; Milligan, D. E. *J. Mol. Spectrosc*. **1975**, *58*, 142.

(17) Zeng, A. H.; Kong, Q. Y.; Wang, Y.; Zhou, M. F. *Chem. Phys*. **2003**, *292*, 111.

(18) Fournier, R. *J. Chem. Phys.* **1993**, *99*, 1801. Fournier, R. *J. Chem. Phys.* **1993**, *98*, 8041. Bauschlicher, C. W., Jr. *J. Chem. Phys*. **1994**, *100*, 1215.

(19) Ogden, J. S. *J. Chem. Soc., Chem. Commun.* **1971**, 978. Huber, H.; Kundig, E. P.; Moskovits, M.; Ozin, G. A. *J. Am. Chem. Soc.* **1975**, *97*, 2097. Kasai, P. H.; Jones, P. M. *J. Am. Chem. Soc*. **1985**, *107*, 813. Chenier, J. H. B.; Hampson, C. A.; Howard, J. A.; Mile, B. *J. Phys. Chem*. **1989**, *93*, 114.

(20) McIntosh, D.; Ozin, G. A. *Inorg. Chem*. **1977**, *16*, 51.

(21) McIntosh, D.; Ozin, G. A. *J. Am. Chem. Soc*. **1976**, *98*, 3167.

(22) Chenier, J. H. B.; Hampson, C. A.; Howard, J. A.; Mile, B. *J. Phys. Chem*. **1988**, *92*, 2745.

(23) Kasai, P. H.; Jones, P. M. *J. Phys. Chem*. **1985**, *89*, 1147. Kasai, P. H.; Jones, P. M. *J. Am. Chem. Soc.* **1985**, *107*, 6385.

(24) Marian, C. M. *Chem. Phys. Lett.* **1993**, *215*, 582.

(25) Manceron, L.; Alikhani, M. E. *Chem. Phys.* **1999**, *244*, 215.

(26) Fournier, R. *J. Chem. Phys.* **1995**, *102*, 5396. Fournier, R. *Int. J. Quantum Chem.* **1994**, *52*, 973.

(27) Tremblay, B.; Gutsev, G.; Manceron, L.; Andrews, L. *J. Phys. Chem. A* **2002**, *106*, 10525.

(28) Tremblay, B.; Manceron, L.; Gutsev, G.; Andrews, L.; Partridge, H. *J. Chem. Phys.* **2002**, *117*, 8479.

(29) Zhou, M. F.; Andrews, L. *J. Phys. Chem. A* **2000**, *104*, 4394.